

Rotational State Distributions of $I_2(B)$ from Vibrational Predissociation of $I_2(B)$ -Ne

Sung-sil Cho and Hosung Sun*

Department of Chemistry and School of Molecular Science (BK21), Sungkyunkwan University, Suwon 440-746, Korea

Received July 7, 2004

The vibrational predissociation of triatomic, *i.e.*, atom-diatom, van der Waals complexes in transient electronic excited state has been widely investigated. The predissociation rates or lifetimes are major concerns of the previous studies. Experimentally rotational state distributions of diatomic product are hardly investigated and few theoretical studies on rotational state distributions have appeared in literature. In this work, choosing the frequently studied $I_2(B)$ -Ne complex as an example, we investigate the change of rotational state distributions of $I_2(B)$ produced from predissociation of the various initial states of $I_2(B)$ -Ne. The present study on the rotational distributions indicates that rotational state distributions depend significantly on the predissociation energy and the van der Waals vibrational modes of $I_2(B)$ -Ne. That is, the initial state dependency of rotational state distributions is extensively discussed.

Key Words : Vibrational predissociation, I_2 -Ne

Introduction

The vibrational predissociation is one of important intramolecular energy transfer (from vibrational to translational energy transfer) phenomena that occur within a molecule having a weak bond. The systems of which vibrational predissociation dynamics is frequently and extensively studied are triatomic (atom-diatom) van der Waals complexes having a typical weak van der Waals bond and one very strong diatomic bond. Particularly (Hal)₂-Rg(= diatomic halogen + rare gas atom) complexes in their excited electronic state are widely studied experimentally and theoretically.^{1,2} A triatomic (Hal)₂-Rg complex can be represented as AB-C (v_1, v_2, v_3) that has three vibrational degrees of freedom. The vibrational quantum number v_1 represents the fast stretching motion of A-B, v_2 is for the van der Waals stretching motion of C with respect to AB, and v_3 is for the van der Waals bending motion of C with respect to AB. The vibrational predissociation process can be viewed as $AB-C(v_1, v_2, v_3) \rightarrow AB(v', j') + C$ where v' is the vibrational quantum number and j' is the rotational quantum number of free diatomic molecule AB. When v' is smaller than v_1 (*i.e.*, $\Delta v (= v' - v_1)$ is negative), vibrational predissociation of AB-C occurs.

Since the early stage of predissociation research,³⁻⁶ the vibrational predissociation of $I_2(B)$ -Ne (in the excited $^3\Pi(0_u^-)$ electronic state⁷) has been most frequently investigated.^{8,24} The first investigation by Levy's group measured predissociation rates and some excited vibrational energy levels of $I_2(B)$ -Ne.³⁻⁶ The accurate vibrational predissociation rates (or lifetimes) of $I_2(B)$ -Ne($v_1, 0, 0$) were first reported by Zewail and coworkers.^{10,11} It is found that the vibrational predissociation rates of $I_2(B)$ -Ne($v_1, 0, 0$) increase as v_1 increases. Recently Heaven and coworkers reported their double resonance studies on $I_2(B)$ -Ne predissociation.^{20,23} So far, experimentally the dissociation energy of $I_2(B)$ -Ne(34, 0, 0) are measured as

53.7 cm⁻¹. For few excited states, *e.g.*, $I_2(B)$ -Ne(34, 1, 0), $I_2(B)$ -Ne(34, 0, 2), $I_2(B)$ -Ne(34, 0, 4), and $I_2(B)$ -Ne(33, 1, 0), etc., the vibrational levels are determined.²³ The predissociation rates for excited (in van der Waals modes) $I_2(B)$ -Ne($v_1, v_2 > 0, v_3 > 0$) are hardly studied while the predissociation of $I_2(B)$ -Ne($v_1, 0, 0$) are investigated for various v_1 . It is also found that the vibrational predissociation process of $\Delta v = -1$ channel, *i.e.*, $I_2(B)$ -Ne($v_1, 0, 0$) $\rightarrow I_2(B, v_1-1) + Ne$, is closed when $v_1 > 36$. The vibrational predissociation through the $\Delta v = -1$ channel is not efficient when $v_1 > 32$.²⁰

Theoretical investigations on vibrational predissociation of $I_2(B)$ -Ne have also been carried out extensively.^{13-19,21,24} The most widely used potential energy function is a pairwise sum of the potentials of diatomic I-I and of Ne-I. The I-I potential energy function is empirically determined from the Zewail's experiment.^{12,17} And the Ne-I potential function is usually taken as a Morse type function whose parameters are fitted to reproduce the experimental predissociation lifetimes of $I_2(B)$ -Ne. Once the potential function is determined, theoretical calculations reveal detailed informations on predissociation, *i.e.*, the predissociation rates, rotational state distributions of product, energy levels including high excited states, etc. The recent theoretical work on $I_2(B)$ -Ne($v_1, 0, 0$) is García-Vela's wave packet calculations.¹⁴ García-Vela suggested a modified potential energy function that is fitted to the above experimental information. And with his modified potential function he calculated the vibrational state distributions, rotational state distributions of product I_2 , and lifetimes of $I_2(B)$ -Ne, etc.

The vibrational predissociations from the van der Waals excited ($v_1, v_2 > 0, v_3 > 0$) levels are also theoretically investigated.²⁴ The calculations reveal that the excitation energies from the ground state to the states with van der Waals bending mode excited (Ne bending around I_2 , *i.e.*, $v_3 > 0$) are smaller than those to the states with stretching mode excited (Ne stretching against I_2 , *i.e.*, $v_2 > 0$). That is, the bending vibrational energy is smaller than that of

*Corresponding Author. e-mail: hsun@skku.edu. Fax: -82-31-290-7075

stretching motion, regardless of the vibrational motion of I-1 stretching (ν_1) vibration. The predissociation rates through $\Delta\nu = -1$ channel are found to be much larger than those through $\Delta\nu = -2$ channel and, consequently, $\Delta\nu = -1$ channel decides the total vibrational predissociation rate. The predissociation rates of the states with van der Waals stretching mode excited are found to be larger than those of the states with bending mode excited, in general. The predissociation rates increase as the stretching motion (ν_1) of I_2 increases because the predissociation energy becomes smaller, regardless of ν_2 or ν_3 . When van der Waals bending mode is excited, the predissociation rates decrease as ν_3 increases. But the predissociation rates increase as the stretching motion (ν_2) between Ne and I_2 increases.

Though a lot of information on the vibrational predissociation of $I_2(B)$ -Ne has been gathered, still a limited knowledge on rotational state distributions of product I_2 has been obtained. Experimentally the rotational state distributions of I_2 produced from the $I_2(B)$ -Ne(32, 0, 0), (33, 0, 0), or (35, 0, 0) predissociation are reported.²⁰ For instance, the predissociation through $\Delta\nu = -1$ channel yields rotational state (j') distribution of product I_2 up to $j' = 17$, while the predissociation through $\nu = -2$ channel yields the distribution up to $j' = 43$. Theoretically a simple fact is known, *i.e.*, the rotational distributions depend strongly on the van der Waals bending mode, while the stretching mode hardly changes the distributions.²⁴

In this work we extensively investigate vibrational predissociation of $I_2(B)$ -Ne ($\nu_1, \nu_2 > 0, \nu_3 > 0$) in excited van der Waals modes using VSCF-DWB-IOS approximation, concentrating on the rotational state distributions of product I_2 . The details of the theoretical method have been reported already.^{18,19} In this method the predissociation is viewed as a half-collision process. Therefore we start our calculation to determine the vibrational wave functions of the bound $I_2(B)$ -Ne in electronically excited B state. To have the bound state wave functions we employ the vibrational self-consistent field approximation (VSCF) of which validity is verified. The continuum state wave function of the dissociating $I_2 +$ Ne should also be evaluated and the infinite-order sudden (IOS) approximation is adopted for this purpose. Then the dissociation rate is evaluated using distorted-wave Born (DWB) approximation that is essentially identical with the well known Fermi's golden rule. This VSCF-DWB-IOS approximation has been found to produce total rates with reasonable accuracy. The quantities we calculated are the predissociation rates of the transient excited vibrational states of $I_2(B)$ -Ne ($\nu_1, \nu_2 > 0, \nu_3 > 0$) and the rotational state distributions of the dissociation product I_2 .

Summary of Theory

The vibrational predissociation of AB-C can be viewed as the dissociation of triatomic complex AB-C(ν_1, ν_2, ν_3) \rightarrow diatomic molecule AB ($\nu' < \nu_1$) and atom C, *i.e.*, AB-C (ν_1, ν_2, ν_3) AB (ν', j') + C. ν_1 is a quantum number for stretching vibration of AB, ν_2 is for stretching van der Waals vibration of C with respect to AB, ν_3 is for bending vibration of C with

respect to AB, ν' is a stretching vibrational quantum number of free AB, and j' is a rotational quantum number of free AB. In this work AB corresponds to I_2 and C to Ne. The VSCF-DWB-IOS approximate method for vibrational predissociation is summarized below. For details, please consult References 18 and 19.

The vector from the center of mass of the diatomic molecule AB to the atom C is denoted R . The distance vector between the atoms A and B is r , and the angle between R and r is θ . The Schrödinger equation for the vibrational motion of AB-C complex can be written as

$$H(r, R, \theta) \Psi(r, R, \theta) = E \Psi(r, R, \theta) \quad (1)$$

The reduced Hamiltonian is

$$H(r, R, \theta) = -\frac{1}{2\mu_1} \frac{\partial^2}{\partial r^2} - \frac{1}{2\mu_2} \frac{\partial^2}{\partial R^2} + \frac{j^2}{2\mu_1 r^2} + \frac{l^2}{2\mu_2 R^2} + V_1(r) + V_2(r, R, \theta) \quad (2)$$

where μ_1 is the reduced mass of A and B, and μ_2 is the reduced mass of diatomic molecule AB and atom C. $V_1(r)$ is the potential energy function between A and B and $V_2(r, R, \theta)$ is the rest of the total potential function, *i.e.*, van der Waals interaction. j and l are the two angular momenta associated with r and R , respectively. When $J = j + l = 0$,

$$j^2 = l^2 = \frac{-1}{\sin \theta} \frac{\partial}{\partial \theta} \left(\sin \theta \frac{\partial}{\partial \theta} \right) \quad (3)$$

The Schrödinger equation (1) is solved for a bound vibrational state AB-C(ν_1, ν_2, ν_3) by using vibrational self-consistent field (VSCF) approximation. The initial (before dissociation) bound state wave function is approximated as,

$$\Psi_{\nu_1, \nu_2, \nu_3}^j(r, R, \theta) \approx \Psi_{\nu_1, \nu_2, \nu_3}^{SCF}(r, R, \theta) \approx \phi_{\nu_1}^1(r) \phi_{\nu_2}^2(R) \phi_{\nu_3}^3(\theta) \quad (4)$$

where

$$H^{SCF}(r, R, \theta) \Psi_{\nu_1, \nu_2, \nu_3}^{SCF}(r, R, \theta) = E_{\nu_1, \nu_2, \nu_3}^{SCF} \Psi_{\nu_1, \nu_2, \nu_3}^{SCF}(r, R, \theta) \quad (5)$$

$$H^{SCF}(r, R, \theta) = h_1(r) + h_2(R) + h_3(\theta) \quad (6)$$

$$h_1(r) \phi_{\nu_1}^1(r) = \varepsilon_{\nu_1}^1 \phi_{\nu_1}^1(r) \quad (7)$$

$$h_2(R) \phi_{\nu_2}^2(R) = \varepsilon_{\nu_2}^2 \phi_{\nu_2}^2(R) \quad (8)$$

$$h_3(\theta) \phi_{\nu_3}^3(\theta) = \varepsilon_{\nu_3}^3 \phi_{\nu_3}^3(\theta) \quad (9)$$

$\varepsilon_{\nu_1}^1, \varepsilon_{\nu_2}^2$, and $\varepsilon_{\nu_3}^3$ are modal eigenvalues for A-B stretching, AB-C van der Waals stretching, and AB-C van der Waals bending motions, respectively. The detailed expressions for H^{SCF} and $H_{\nu_1, \nu_2, \nu_3}^{SCF}$ are not presented here for brevity.^{18,19}

Now we determine a final continuum (or dissociating) state wave function, $\Psi_{\nu', j'}^f(r, R, \theta)$. Here we use a vibrationally adiabatic approximation, which is

$$\Psi_{v',j'}^f(r, R, \theta) \approx \phi_{v'}^d(r) \phi_{j'}^E(R, \theta) \quad (10)$$

where $\phi_{v'}^d(r)$ is the stretching vibrational wave function of the state v' of free AB. The continuum wave function $\phi_{j'}^E(R, \theta)$ consists of two parts: one is the rotational (j') motion of AB and the other is a relative translational (E) motion of AB with respect to C. The Schrödinger equation for $\phi_{j'}^E(R, \theta)$ is

$$\left[-\frac{1}{2\mu_2} \frac{\partial^2}{\partial R^2} + \frac{1}{2\mu_2 R^2} \mathbf{l}^2 + \langle \phi_{v'}^d(r) | \frac{1}{2\mu_1 r^2} | \phi_{v'}^d(r) \rangle \mathbf{j}^2 \right. \\ \left. + \langle \phi_{v'}^d(r) | V_2(r, R, \theta) | \phi_{v'}^d(r) \rangle - (E_{v_1, v_2, v_3}^i - E_{v'}^d) \right] \phi_{j'}^E(R, \theta) = 0 \quad (11)$$

where $E_{v'}^d$ is the v' vibrational energy of free AB.

Under IOS, we set $\mathbf{j}^2 = \mathbf{l}^2 = j'(j' + 1)$ because the total angular momentum is fixed as zero, then the scattering equation we have to solve is one-dimensional, *i.e.*,

$$\left[-\frac{1}{2\mu_2} \frac{\partial^2}{\partial R^2} + \frac{1}{2\mu_2 R^2} j'(j' + 1) + B j'(j' + 1) \right. \\ \left. + \bar{V}_2(R; \theta) - E \right] \phi_{j'}^E(R; \theta) = 0 \quad (12)$$

where B is a rotational constant of AB at the state v' [the third term in Eq. (11)], $\bar{V}_2(R; \theta)$ is the averaged V_2 integral over $\phi_{v'}^d(r)$ [the fourth term in Eq. (11)], E is the translational energy which is $E_{v_1, v_2, v_3}^i - E_{v'}^d$, and $\phi_{j'}^E(R; \theta)$ parametrically depends on angle θ .

The dissociation process is assumed to be due to mode-mode coupling which causes energy transfer (and predissociation) from vibrational motion of AB-C to kinetic motion of C ($V \rightarrow T$). The coupling, $V_c (= H - H^{\text{SCF}})$ is generally so weak that a perturbative approach could be suitable (DWB approximation). The vibrational predissociation rate R is, when the energy normalized continuum wave function $\Psi_{v',j'}^f(r, R, \theta)$ is used,

$$R(v_1 v_2 v_3 \rightarrow v' j') = 2\pi \langle | \Psi_{v',j'}^f(r, R, \theta) | V_c | \Psi_{v_1 v_2 v_3}^i(r, R, \theta) \rangle^2 \quad (13)$$

The rotational state population $P(v_1 v_2 v_3 \rightarrow v' j')$, in units of %, of AB (v', j') from AB-C ($v_1 v_2 v_3$) is,

$$P(v_1 v_2 v_3 \rightarrow v' j') = R(v_1 v_2 v_3 \rightarrow v' j') / \sum_j R(v_1 v_2 v_3 \rightarrow v' j') \times 100 \quad (14)$$

The total predissociation rate $R(v_1 v_2 v_3)$ from AB-C (v_1, v_2, v_3) to AB(v', j') + C is

$$R(v_1 v_2 v_3) = \sum_v \sum_j R(v_1 v_2 v_3 \rightarrow v' j') \quad (15)$$

Computations and Results

The best known potential energy function for I₂(B)-Ne is

$$V(r, R, \theta) = V_{I-1}(r) + 2V_{I-Ne}(r, R, \theta) + C(v_1) \quad (16)$$

The analytical form of I-I potential function for I₂(B), $V_{I-1}(r)$

is obtained from the Gruebele and Zwail's experiment.^{12,17} García-Vela¹⁴ suggested a new Morse type potential function for I-Ne, $V_{I-Ne}(r, R, \theta)$ in which parameters are fitted to the experimental dissociation energy of I₂(B)-Ne(34, 0, 0). The extra term $C(v_1)$, which depends on the I-I stretching vibrational motion, is introduced to exactly reproduce both experimental dissociation energies of I₂(B)-Ne(0, 0, 0) and I₂(B)-Ne(34, 0, 0) simultaneously.²⁴ The potential energy function produces the equilibrium geometry of I₂(B)-Ne as T-shaped which is experimentally found in Burroughs *et al.*'s experiment.²⁰ From now on I₂(B)-Ne(v_1, v_2, v_3) is briefly written as I₂-Ne(v_1, v_2, v_3) or (v_1, v_2, v_3).

The vibrational state energies of I₂-Ne(v_1, v_2, v_3) are calculated using the suggested VSCF method where relevant equations (Eqs. 7, 8, and 9) are numerically and iteratively solved. For the \mathbf{r} coordinate, the numerical integration was performed with the grid size of 0.001 au from $r = 4.5$ to 15 au. For the \mathbf{R} , the grid size is 0.05 au from $R = 5$ to 40 au. It guarantees that the starting point of integration is well inside the classically forbidden region and at a large distance, the bound state wave function converges to zero and the continuum wave function becomes a plane wave, *i.e.*, free from the interaction. For the angle (θ) variable, the discrete variable representation is adopted and the 100 Legendre functions, that is, 100 grid points are used. The 127 amu isotope of I and the 20 amu Ne are assumed. With the same numerical quadrature the dissociating state wave functions are calculated. The vibrational wave functions of free I₂ are numerically solved and the continuum wave function of outgoing product I₂ has been determined using the IOS approximation (Eq. 12). The Eq. 12 is solved repeatedly at 100 angles. Under the DWB approximation, the predissociation rates of I₂-Ne(v_1, v_2, v_3) and the rotational state distributions of I₂(v', j') are evaluated using Eqs. 13 and 14.

The vibrational energy levels of I₂-Ne(v_1, v_2, v_3) are well studied previously.²⁴ The level structures are, in general, ($v_1, 0, 0$) < ($v_1, 0, 1$) < ($v_1, 0, 2$) < ($v_1, 1, 0$) < ($v_1, 0, 3$) < ($v_1, 1, 1$) < ($v_1, 1, 2$) < ($v_1, 2, 0$) < ($v_1, 1, 3$) < ($v_1, 2, 1$) < ($v_1, 2, 2$) in the order of increasing energies. Of course the vibrational energy levels of I₂($v', j' = 0$) are almost exactly known.¹² The predissociation can be viewed as the reaction of I₂-Ne(v_1, v_2, v_3) \rightarrow I₂(v', j') + Ne. When $\Delta v (= v' - v_1) = -1$, it is called the $\Delta v = -1$ process (or channel). And the $\Delta v = -2$ channel when $\Delta v = -2$, etc. The reaction energy for the dissociation can be called the predissociation energy PE that is equal to Energy[I₂-Ne(v_1, v_2, v_3)] - Energy[I₂($v', j' = 0$)]. When PE are positive, the dissociation occurs spontaneously.

As mentioned in the Introduction section, the studies on predissociation dissociation of I₂-Ne($v_1, 0, 0$) have been reported by many authors. In Table 1, the predissociation rates (Rates) and predissociation energies (PE) of I₂-Ne($v_1, 0, 0$) through $\Delta v = -1$ channel are listed. From the Table 1, we see that the vibrational predissociation rates of ($v_1, 0, 0$) increase as v_1 increases (energy gap law), which is consistent with previous studies. The energy gap law is due to the fact that the PE decreases as v_1 increases. As v_1 becomes larger, the level gap between adjacent two v_1 levels of I₂ in I₂-Ne

Table 1. Vibrational predissociation rates (Rates in 10^9s^{-1}), predissociation energies (PE in cm^{-1}), and rotational constants of $\text{I}_2(v_1-1)$ ($B(v_1-1)$ in cm^{-1}) from $\text{I}_2\text{-Ne}(v_1, 0, 0) \rightarrow \text{I}_2(v_1-1, j') + \text{Ne}$. In rotational state distributions of product $\text{I}_2(v_1-1, j')$ three characteristic rotational quantum numbers, *i.e.*, j'_{largest} , j'_{max} , and j'_{peak} are found

v_1	Rates	PE	$B(v_1-1)$	j'_{largest}	j'_{max}	j'_{peak}
1	0.28	59.54	0.0289	44	38	20
5	1.01	54.18	0.0283	42	38	20
10	2.73	46.88	0.0275	40	36	20
15	5.74	39.00	0.0265	36	34	18
20	12.95	30.61	0.0255	34	30	18
23	18.52	25.36	0.0248	32	28	2
26	37.56	20.00	0.0241	26	26	2
29	51.83	14.54	0.0233	24	22	2
33	109.77	7.20	0.0225	18	18	2
34	122.33	5.35	0.0220	14	14	2
36	178.25	1.69	0.0214	8	8	2
37	closed	-0.14	-	-	-	-

becomes smaller. And it makes the energy difference between $\text{I}_2\text{-Ne}(v_1, 0, 0)$ and free $\text{I}_2(v_1-1)$ smaller so that the dissociation from $\text{I}_2\text{-Ne}$ to $\text{I}_2 + \text{Ne}$ becomes faster. The PE for $\text{I}_2\text{-Ne}(37, 0, 0)$ in Table 1 is negative so that the predissociation through $\Delta v = -1$ channel should not occur for $\text{I}_2\text{-Ne}(37, 0, 0)$, which is consistent with experimental finding.^{2,20} Our calculated rotational constants of I_2 at various vibrational levels, *i.e.*, $B(v_1-1)$, are also listed in Table 1. The rotational constant becomes smaller as v_1 increases. It reflects that the bond length becomes longer as I_2 has larger vibrational energy.

The largest rotational energy that product I_2 can have, of course, is equal to the predissociation energy PE. This rotational state is denoted as a quantum number j'_{largest} in Table 1. The j'_{largest} is the largest integer that satisfies the relation, *i.e.*, $B(v_1-1) * j'_{\text{largest}} * (j'_{\text{largest}} + 1) \leq \text{PE}$. Since theoretical calculations enable one to calculate the $B(v_1-1)$ and PE, we could determine j'_{largest} . As shown in Figure 1, the rotational state distributions of I_2 end at a certain rotational quantum number (j'_{max}). (The criterion to choose j'_{max} is that the total population (%) of all rotational states whose rotational quantum number is larger than j'_{max} should be smaller than 0.01%.) The j'_{max} are listed in Table 1. Of course the j'_{max} are the highest rotational state that I_2 can carry. The j'_{max} should be equal to j'_{largest} energetically, but it is found that j'_{max} are, in most cases, smaller than j'_{largest} . It is due to a dynamical effect, *e.g.*, the overlap between the bound state wave function and the dissociating state wave function. Therefore j'_{largest} (or j'_{max}) decreases as v_1 increases. That is, I_2 produced from the predissociation of higher v_1 states of $\text{I}_2\text{-Ne}(v_1, 0, 0)$ has less rotational energy, *i.e.*, rotates slowly.

Heaven and coworkers²⁰ experimentally determined that the j'_{max} of $\text{I}_2(v' = 31, j')$ produced from the predissociation of $\text{I}_2\text{-Ne}(32, 0, 0)$ is 17 and its recoil energy is 2.6 cm^{-1} . In Table 1 we see that our calculated j'_{max} is 18. Odd or even number of rotational quantum number is not a matter of

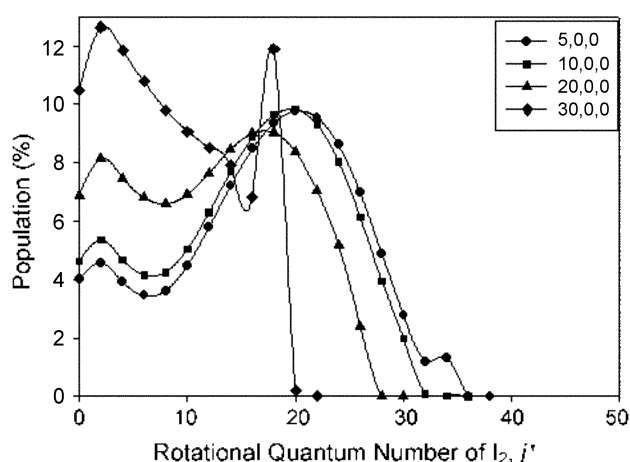


Figure 1. Rotational state distributions of $\text{I}_2(v_1-1, j')$ from $\text{I}_2\text{-Ne}(v_1, 0, 0) \rightarrow \text{I}_2(v_1-1, j') + \text{Ne}$ where $v_1 = 5, 10, 20,$ or 30 .

concern but rather it is a matter of choice because I_2 is homonuclear. Our value of 18 corresponds to 17 if odd number was chosen. Then our calculated recoil energy is $\text{PE} - B * j'_{\text{max}} * (j'_{\text{max}} + 1)$, *i.e.*, $9.04 - 0.0225 * 17 * (17 + 1) = 2.16 \text{ cm}^{-1}$ that is comparable to experimental value of 2.6 cm^{-1} . Garcia-Vela's wave packet calculations¹⁴ also showed j'_{max} is 18. Here theory and experiment agree to each other very well.

In Figure 1, the rotational state distributions of $\text{I}_2(v_1-1, j')$ produced from the vibrational predissociation reaction of $\text{I}_2\text{-Ne}(v_1, 0, 0) \rightarrow \text{I}_2(v_1-1, j') + \text{Ne}$ ($v_1 = 5, 10, 20,$ and 30) are presented. As we see in all cases, the distributions exhibit two distinct maximum peaks, *i.e.* bimodal. This bimodal structure appearing in vibrational predissociation of triatomic complexes was well analyzed by Lee using the concept of angle functions.^{25,26} We do not repeat the analysis here but want to stress that the angle(θ) dependence of the first derivative of the potential energy function (between I_2 and Ne) plays a key role in rotational state distributions of product I_2 .

The rotational quantum number of the larger peak among the two maxima in rotational state distributions of I_2 is denoted as j'_{peak} . From Figure 1, we note that the j'_{peak} is 20 from (5, 0, 0), 20 from (10, 0, 0), 18 from (20, 0, 0), and 2 from (30, 0, 0). We also see that the peak at small j' becomes larger and larger as v_1 increases from $v_1 = 5$ to 30. And at $v_1 = 30$, the peak at small j' ($= 2$) is eventually larger than the peak at large j' ($= 18$). This observation can be explained in three folds. i) The predissociation reaction energy PE decreases as v_1 increases. Consequently the energy that the product I_2 can carry becomes smaller so that the rotational energy of I_2 becomes naturally smaller. ii) Furthermore, the predissociation rate increases as v_1 increases. At high v_1 , the dissociation occurs so fast that the orientation of the leaving I_2 is not much different from that in the complex $\text{I}_2\text{-Ne}$ where the total rotational motion (J) is zero. iii) Finally, based on Lee's analysis,²⁶ the effective potential (averaged over the I-I distance coordinate r) that governs the dissociation becomes smoother as v_1 increases. Therefore the anisotropy of potential decreases, *i.e.*, the potential becomes shallow over the angle

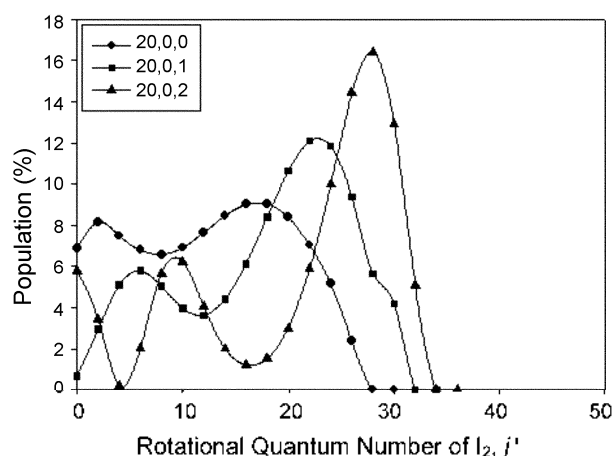


Figure 2. Rotational state distributions of I₂(19, *j'*) from I₂-Ne(20, *v*₂, *v*₃) → I₂(19, *j'*) + Ne where (*v*₁, *v*₂, *v*₃) = (20, 0, 0), (20, 0, 1), or (20, 0, 2).

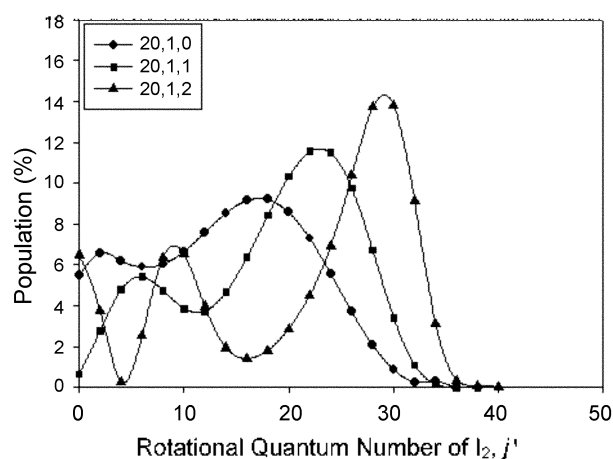


Figure 3. Rotational state distributions of I₂(19, *j'*) from I₂-Ne(20, *v*₂, *v*₃) → I₂(19, *j'*) + Ne where (*v*₁, *v*₂, *v*₃) = (20, 1, 0), (20, 1, 1), or (20, 1, 2).

coordinate θ . It, of course, does not alter the rotational motion of the leaving I₂ significantly. The j'_{peak} from various I₂-Ne(*v*₁, 0, 0) states are listed in Table 1.

The rotational state distributions of I₂(*v'* = 19, *j'*) produced from the predissociation of various (20, *v*₂, *v*₃) states are presented in Figures 2, 3, and 4. Again they exhibit the bimodal structures. We note that the distribution from (20, 0, 0) is almost identical with that from (20, 1, 0) or (20, 2, 0). The same is true for the case from (20, 0, 1)/(20, 1, 1)/(20, 2, 1) or (20, 0, 2)/(20, 1, 2)/(20, 2, 2). From this we learn that the change in van der Waals stretching mode does not alter the rotational state distributions of product I₂, as expected. But the change in bending mode drastically changes the distributions. For example, see the (20, 0, 0), (20, 0, 1) and (20, 0, 2) distributions in Figure 2. The states in higher bending mode produce more rotationally hot I₂ diatomic molecules. That is, the maximum peak (j'_{peak}) appears at a higher rotational quantum number of I₂. Naturally the large bending motion of Ne with respect

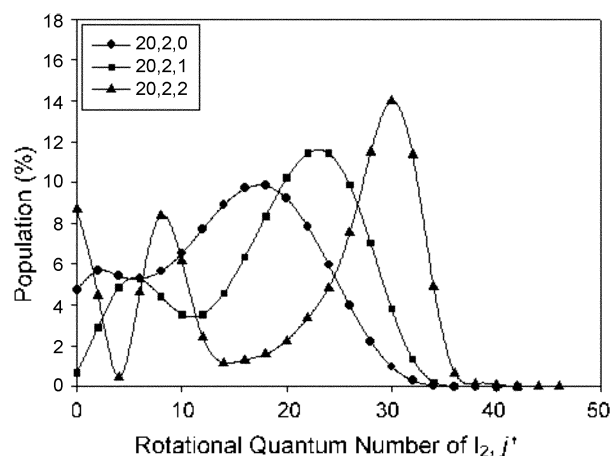


Figure 4. Rotational state distributions of I₂(19, *j'*) from I₂-Ne(20, *v*₂, *v*₃) → I₂(19, *j'*) + Ne where (*v*₁, *v*₂, *v*₃) = (20, 2, 0), (20, 2, 1), or (20, 2, 2).

Table 2. The j'_{peak} in rotational state distributions of product I₂(*v*₁-1) from I₂-Ne(*v*₁, *v*₂, *v*₃) → I₂(*v*₁-1, *j'*) + Ne

<i>v</i> ₁	(<i>v</i> ₁ , 0, 1)	(<i>v</i> ₁ , 0, 2)	(<i>v</i> ₁ , 1, 0)	(<i>v</i> ₁ , 1, 1)	(<i>v</i> ₁ , 1, 2)	(<i>v</i> ₁ , 2, 0)	(<i>v</i> ₁ , 2, 1)	(<i>v</i> ₁ , 2, 2)
1	27	30	20	27	30	22	27	32
5	27	30	20	27	30	22	27	32
10	25	30	20	27	30	20	27	32
15	25	28	18	25	30	18	25	30
20	23	28	18	23	30	18	25	30
23	23	28	16	23	28	16	23	30
26	21	26	2	21	28	14	21	28
29	21	26	2	21	26	14	21	12
34	9	12	2	19	12	2	19	12
36	9	12	2	19	12	2	19	12
37	9	12	2	19	12	2	19	12
40	9	12	2	15	12	2	19	12
43	closed	12	2	11	12	2	17	12

to I₂ should bring about the high rotational motion of I₂.

We find the same trend in rotational state distributions of I₂ from other van der Waals excited states of I₂-Ne(*v*₁, *v*₂ > 0, *v*₃ > 0) as listed in Table 2. As *v*₁ increases, the j'_{peak} from excited (*v*₁, *v*₂ > 0, *v*₃ > 0) state decreases as the j'_{peak} from (*v*₁, 0, 0) does. That is, the diatomic molecule I₂ produced from the predissociation of high (*v*₁ is large) vibrational state is mostly in low rotational state.

So far our discussion is limited to the $\Delta v = -1$ channel, *i.e.*, I₂-Ne(*v*₁, *v*₂, *v*₃) → I₂(*v*₁-1, *j'*) + Ne. We have performed the same calculations for other channels, *i.e.*, $\Delta v = -2$, and -3 , etc. It is found that the rotational state distributions of product I₂ through $\Delta v = -1$ channel are notably different from those through $\Delta v = -2$ channel.^{14,24} But, here we do not present analyses on the distributions through higher channels because the $\Delta v = -2$ or up channels do not contribute much to the total predissociation rate. The predissociation rates for $\Delta v = -2$ are one or two orders of magnitude smaller than the $\Delta v = -1$, and the $\Delta v = -3$ rates are even smaller than the $\Delta v = -2$.²⁴

Summary and Conclusion

The direct vibrational predissociation of $I_2(B)$ -Ne(v_1, v_2, v_3) in ground and excited vibrational states has been theoretically investigated by using the fast and simple quantum mechanical VSCF-DWB-IOS method. The work concentrated on the rotational state distributions of I_2 produced from various (v_1, v_2, v_3) states. The summary of the work is as follows:

i) The vibrational levels of $I_2(B)$ -Ne(v_1, v_2, v_3) are determined. The level structures are, in general, ($v_1, 0, 0$) < ($v_1, 0, 1$) < ($v_1, 0, 2$) < ($v_1, 1, 0$) < ($v_1, 0, 3$) < ($v_1, 1, 1$) < ($v_1, 1, 2$) < ($v_1, 2, 0$) < ($v_1, 1, 3$) < ($v_1, 2, 1$) < ($v_1, 2, 2$) in the order of increasing energies. ii) The predissociation rates increase as the stretching motion (v_1) of I_2 increases, regardless of v_2 or v_3 (energy gap law). A similar energy gap law is found when the van der Waals bending motion changes, *i.e.*, the predissociation rates decrease as the van der Waals bending motion (v_3) increases. But the predissociation rates increase as the van der Waals stretching motion (v_2) between Ne and I_2 increases. iii) The rotational state distributions of I_2 produced from the vibrational predissociation of I_2 -Ne exhibit two distinct maximum peaks, *i.e.* bimodal.

The above three findings have been reported before and we verified them in this work. The new findings are: iv) The change in van der Waals stretching mode does not alter the rotational state distributions of product I_2 . But the change in bending mode drastically changes the distributions. v) The maximum peak in rotational state distributions of product I_2 moves to a lower rotational quantum number region as v_1 increases. That is, the I_2 produced from the predissociation of $I_2(B)$ -Ne(v_1, v_2, v_3) at high (v_1 is large) vibrational state carries very little rotational energy.

The advantage of the proposed method lies in capability of exactly locating the transient complex's ($I_2(B)$ -Ne in this work) vibrational level. It enables one to easily study the vibrational predissociation of the complex in vibrationally excited van der Waals mode that can not be easily investigated by using other theoretical methods.

Acknowledgements. This work was supported by Korea Research Foundation Grant (KRF-2002-070-C00048).

References

1. Rohrbacher, A.; Halberstadt, N.; Janda, K. C. *Ann. Rev. Phys. Chem.* **2000**, *51*, 405.
2. Buchachenko, A. A.; Halberstadt, N.; Lepetit, B.; Roncero, O. *Int. Rev. Phys. Chem.* **2003**, *22*, 153.
3. Kubiak, G.; Fitch, P. S. H.; Wharton, L.; Levy, D. H. *J. Chem. Phys.* **1978**, *68*, 4477.
4. Sharfin, W.; Johnson, K. E.; Wharton, L.; Levy, D. H. *J. Chem. Phys.* **1979**, *71*, 1292.
5. Kenny, J. E.; Johnson, K. E.; Sharfin, W.; Levy, D. H. *J. Chem. Phys.* **1980**, *72*, 1109.
6. Blazy, J. A.; DeKoven, B. M.; Russell, T. D.; Levy, D. H. *J. Chem. Phys.* **1980**, *72*, 2439.
7. Asano, Y.; Yabushita, S. *Bull. Korean Chem. Soc.* **2003**, *24*, 703.
8. Schatz, G. C.; Gerber, R. B.; Ratner, M. A. *J. Chem. Phys.* **1988**, *88*, 3709.
9. Garcia-Vela, A.; Villarreal, P.; Delgado-Barrio, G. *J. Chem. Phys.* **1991**, *94*, 7868.
10. Willberg, D. M.; Guttman, M.; Breen, J. J.; Zewail, A. H. *J. Chem. Phys.* **1992**, *96*, 198.
11. Guttman, M.; Willberg, D. M.; Zewail, A. H. *J. Chem. Phys.* **1992**, *97*, 8037.
12. Gruebele, M.; Zewail, A. H. *J. Chem. Phys.* **1993**, *98*, 883.
13. Rubayo-Soneira, J.; Garcia-Vela, A.; Villarreal, P.; Delgado-Barrio, G. *Chem. Phys. Lett.* **1995**, *243*, 236.
14. Garcia-Vela, A. *J. Chem. Phys.* **1996**, *104*, 1047.
15. Buchachenko, A. A. *Chem. Phys. Lett.* **1998**, *292*, 273.
16. Seong, J.; Sun, H. *Bull. Korean Chem. Soc.* **1998**, *19*, 539.
17. Bastida, A.; Zuñiga, J.; Requena, A.; Halberstadt, N.; Beswick, J. A. *J. Chem. Phys.* **1998**, *109*, 6320.
18. Jung, J.; Sun, H. *Chem. Phys. Lett.* **2001**, *336*, 311.
19. Jung, J.; Sun, H. *Mol. Phys.* **2001**, *99*, 1867.
20. Burroughs, A.; Kerenskaya, G. K.; Heaven, M. C. *J. Chem. Phys.* **2001**, *115*, 784.
21. Garcia-Vela, A. *J. Phys. Chem. A* **2002**, *106*, 6857.
22. Jung, J.; Sun, H. *Bull. Korean Chem. Soc.* **2002**, *23*, 245.
23. Heaven, M. C.; Buchachenko, A. A. *J. Mol. Spectrosc.* **2003**, *222*, 31.
24. Cho, S.; Sun, H. *Chem. Phys. Lett.* **2003**, *377*, 406.
25. Lee, C.-W. *Bull. Korean Chem. Soc.* **1995**, *16*, 957.
26. Lee, C.-W. *Bull. Korean Chem. Soc.* **1995**, *16*, 1193.